Journal of Ovonic Research Vol. 15, No. 6, November-December 2019, p. 377 - 385

INFLUENCE OF SUBSTRATE TEMPERATURE AND THICKNESS ON STRUCTURAL AND OPTICAL PROPERTIES OF CZTS NANOSTRUCTURES THIN FILMS

Z. T. KHODAIR[a], N. A. BAKR[a], A. M. HASSAN[b], A. A. KAMIL[a]
[a]*Department of Physics, College of Science, University of Diyala, Diyala, Iraq*
[b]*Directorate-General for Education Diyala, Iraq*

In this research, Cu_2ZnSnS_4 (CZTS) nanostructures thin films were deposited on glass substrates at different substrate temperatures (300, 350 and 400 ^oC) and thicknesses (140, 425 and 530 nm) by chemical spray pyrolysis. Optical and structural analyses of all the films were conducted by means of UV-VIS-NIR spectroscopy and XRD. The CZTS films were found to have a maximum crystallite size ranging between 11.71 nm and 15.47 nm at 350 ^oC and 530 nm of substrate temperature and thickness, respectively. The transmittance increased with an increase in the substrate temperature and decreased with increasing thickness. The optical energy gap value decreased with increasing substrate temperature and increased with increasing thickness. The optical constants were calculated.

(Received August 22, 2019; Accepted November 14, 2019)

Keywords: CZTS thin films, Structural properties, Optical properties, XRD

1. Introduction

Copper zinc tin sulphide (Cu_2ZnSnS_4) thin film is a promising and low-cost film for solar cells [1]. Cu_2ZnSnS_4 is a semiconductor material with a direct energy band gap, and The effect of temperature on Cu_2ZnSnS_4 band gap for applications solar cell that are affected by daily temperature variations [2, 3]. It can be formed by RF sputtering and vapour phase sulfurization [4], electrodeposition, hybrid reactive sputtering, nanocrystal ink deposition, pulsed laser deposition (PLD), photochemical deposition, Atmospheric pressure chemical vapor deposition and spray pyrolysis [1, 5]. Cu_2ZnSnS_4 is one of the most promising absorber materials for low-cost solar cell thin films. It has a high absorption coefficient and a direct band gap which about($\geq 10^4$ cm^{-1}) and 1.5 eV) respectively [6]. In this report, the structural and optical properties of Cu_2ZnSnS_4 deposited on glass substrates using the CSP (chemical spray pyrolysis) method at various substrate temperatures and thicknesses were studied.

2. Materials and method

The spray pyrolysis technique was employed to prepare Cu_2ZnSnS_4 thin films at different temperatures (300, 350 and 400 ^oC) and thicknesses (140, 425 and 530 nm). The precursor solution was achieved by mixing of CuCl (0.04 mol/L), $ZnCl_2$, (0.02 mol/L), $SnCl_4$. $5(H_2O)$ (0.02 mol/L) and SC $(NH_2)_2$ (0.18 mol/L) as aqueous solutions to obtain a final volume of 100 ml. The elemental ratio of Cu/Zn/Sn/S for the preparation of the thin films was 2/1/1/8 in the solution. The experiments were conducted at various substrate temperatures (300, 350 and 400 ^oC) and thicknesses (140, 425 and 530 nm). The thickness of the deposited film was measured by the conventional gravimetric technique. The resulting solution was sprayed onto the glass substrates.

3. Results

3.1. XRD analysis

The XRD results all the Cu_2ZnSnS_4 films are shown in Fig. 1. The patterns were recorded in the range of 2θ~28.50, referred to as (112), which was in agreement with the ICDD card number, 26-0575. The XRD pattern revealed that the deposited films were polycrystalline in nature with a tetragonal structure, and this was in good agreement with the reported data on the structure of Cu_2ZnSnS_4 [7, 8]. It could be seen that when the substrate temperature was increased from 300 ^oC to 350 ^oC, the "2θ" position for the (112) direction shifted to a higher value, whereas at 400 ^oC it shifted to a lower value, as shown in Table (1). It could be seen that the 2θ position for the (112) direction at a thickness of 140 nm had a higher value, as shown in Table (2). In addition, the lattice constants (a and c) for Cu_2ZnSnS_4 increased with increasing substrate temperature and thickness, respectively, as shown in Table (2), where the prepared film had (a and c) values that were nearest to the standard lattice constants. These results were in agreement with those of previous studies as the theoretical values were (a = 5.42 Å) and (c = 10.848Å) [8, 9]. The average crystallite size (D_{av}) in nm was estimated for the (112) plane by using the Scherrer method [10]:

$$D_{av} = \frac{K\,\lambda}{\beta \cos\theta} \quad (1)$$

where K is a constant (0.9), λ is the wavelength of the X-ray radiation, β is in radians, and θ is the Bragg's diffraction angle. The maximum range was ~11.715 to 15.4724 nm for the films prepared at a substrate temperature of 350 ^oC and thickness of 530 nm, which was in agreement with the findings of other studies [7 - 9]. The higher crystallite size values indicated more crystallization of the films, and its noticed that the average of crystallite size of all Cu_2ZnSnS_4 films in nanostructure range.

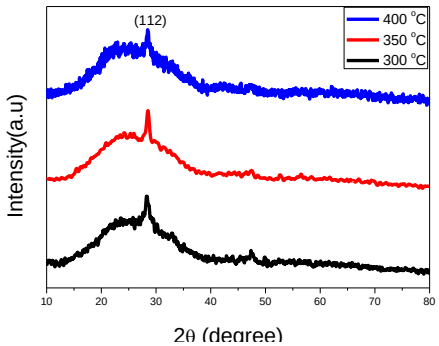

Fig. 1. (a) XRD analysis of Cu_2ZnSnS_4 at different substrate temperatures.

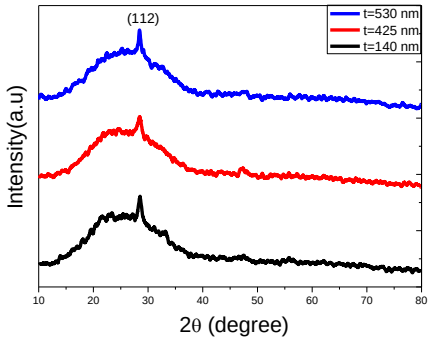

Fig 1. (b) XRD analysis of Cu_2ZnSnS_4 at different thicknesses.

The texture coefficient (T_c) symbolizes the texture of a particular plane. The T_c of all the films were estimated by using [11]:

$$T_C(hkl) = \frac{I(hkl)/I_0(hkl)}{N_r^{-1}\Sigma I(hkl)/I_o(hkl)} \quad (2)$$

where: I_o(hk*l*) is the intensity of the ICDD, I(hk*l*) is the measured intensity, N_r is the number of reflections. The T_c (*hkl)* was calculated for the (112) plane of the thin films. The values of T_c were >1 for all the samples, thereby indicating that there were numerous grains in the (112) plane.

Table 1. XRD analysis of Cu_2ZnSnS_4 at different substrate temperatures.

Substrate Temperature T (^oC)		300	350	400
2Θ (deg)		28.445	28.5353	28.462
hkl		(112)	(112)	(112)
d (Å)		3.1352	3.12556	3.1282
(FWHM) (deg)		0.80	0.70	0.71
(D_{av}) nm		10.25	11.71	11.50
Lattice Constants (Å)	a	5.404	5.419	5.420
	c	10.976	10.86	10.541
T_c		1.720	1.923	1.810

Table 2. XRD analysis of Cu_2ZnSnS_4 at different thicknesses.

Thicknesst (nm)		140	425	530
2Θ (deg.)		28.5253	28.4820	28.5103
hkl		(112)	(112)	(112)
d (Å)		3.1266	3.1312	3.1282
(FWHM) (deg)		0.720	0.753	0.530
(D_{av}) nm		11.39	10.89	15.47
Lattice Constants(Å)	a	5.433	5.434	5.731
	c	10.752	10.816	9.843
T_c		1.546	1.667	1.694

3.2. Optical Properties

A UV–visible spectrophotometer was used to record the optical absorption spectra for the samples within the spectral range of about 300 - 900 nm. Figures (2a) and (2b) show the wavelength transmittance at changing substrate temperatures and different thicknesses. The

transmittance increased with increasing substrate temperature and decreased with increasing thickness.

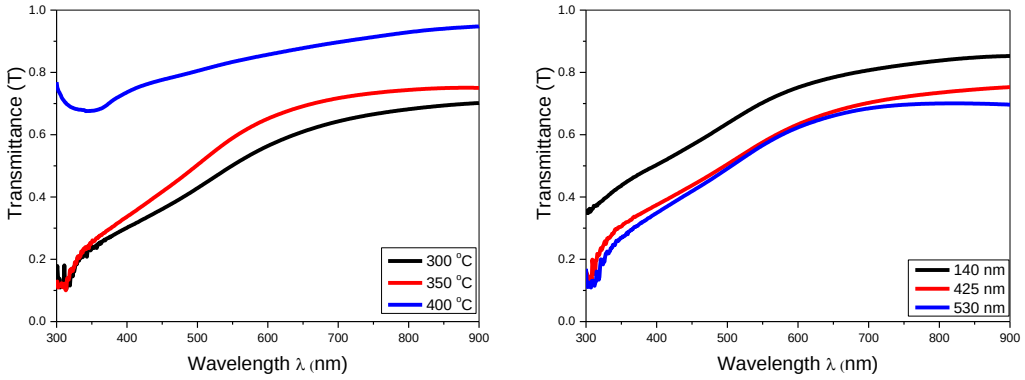

Fig. 2. Transmittance (T) of Cu_2ZnSnS_4 films (a) at different substrate temperatures, and (b) at different thicknesses.

Figs. (3a) and (3b) show the absorbance (A) with variations in the wavelength for Cu_2ZnSnS_4 films at different substrate temperatures and thicknesses. It was noticed that the absorbance decreased with increasing substrate temperature and thickness.

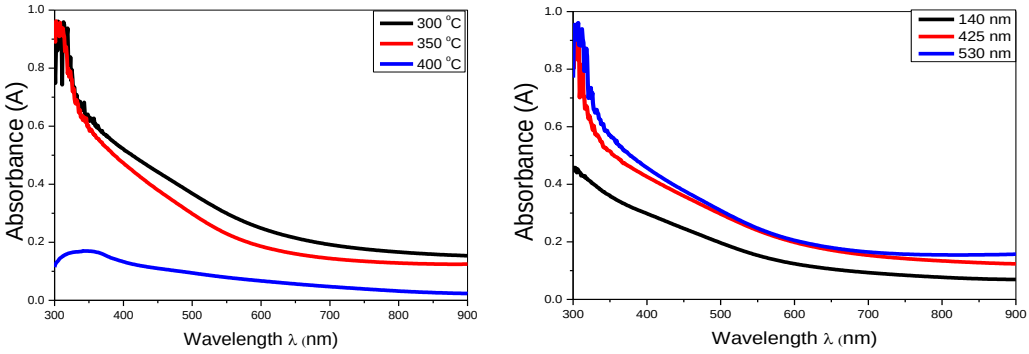

Fig. 3. Absorbance (A) of Cu_2ZnSnS_4 films at (a) different substrate temperatures, and (b) at different thicknesses.

The absorption coefficient α was estimated by using [12]:

$$\alpha = (2.303 \times A) / t \quad (2)$$

where t is the thickness of the thin films, A is the absorbance. It was observed that all the samples had a high absorption coefficient in the visible range of the solar spectrum, as shown in Fig. 4. The absorption coefficient increased with an increase in the photon energy and was larger than 10^4 cm^{-1}, which denoted an increase in the probability of the presence of direct transitions. It could be seen that the absorption coefficient decreased as the substrate temperature and thickness increased.

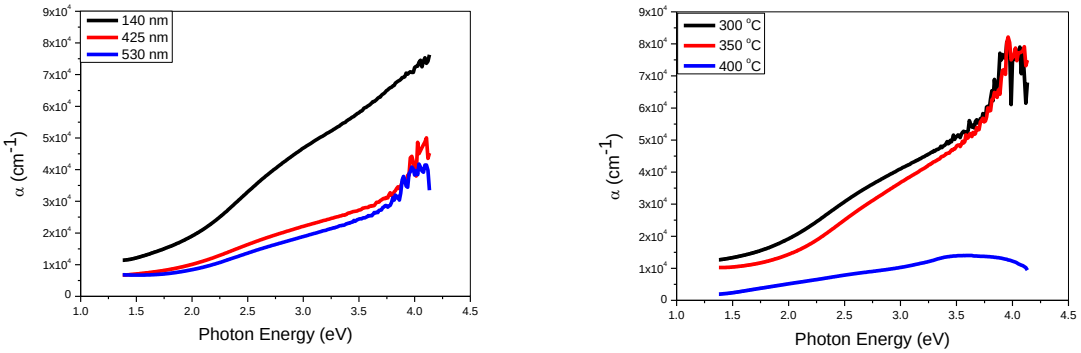

a) *b)*

Fig. 4. Absorption coefficient of Cu_2ZnSnS_4 films (a) at different substrate temperatures, and (b) at different thicknesses.

The absorption coefficient showed a tail corresponding to the so-called Urbach tail for the sub-band gap photon energy. This was related to the disorder in the crystalline lattice film, and was estimated by [10]

$$\alpha = \alpha_o \exp(\frac{h\nu}{Eu}) \tag{3}$$

where α_o is the constant, and E_u is the Urbach energy.

Figs. (5) and (6) show the difference (lnα) against the photon energy . The value of E_u was estimated as the reciprocal of the straight line slope, as displayed in the figures. It was noticed that the Urbach energy tended to decrease as the substrate temperature and thickness increased, as shown in Table 3.

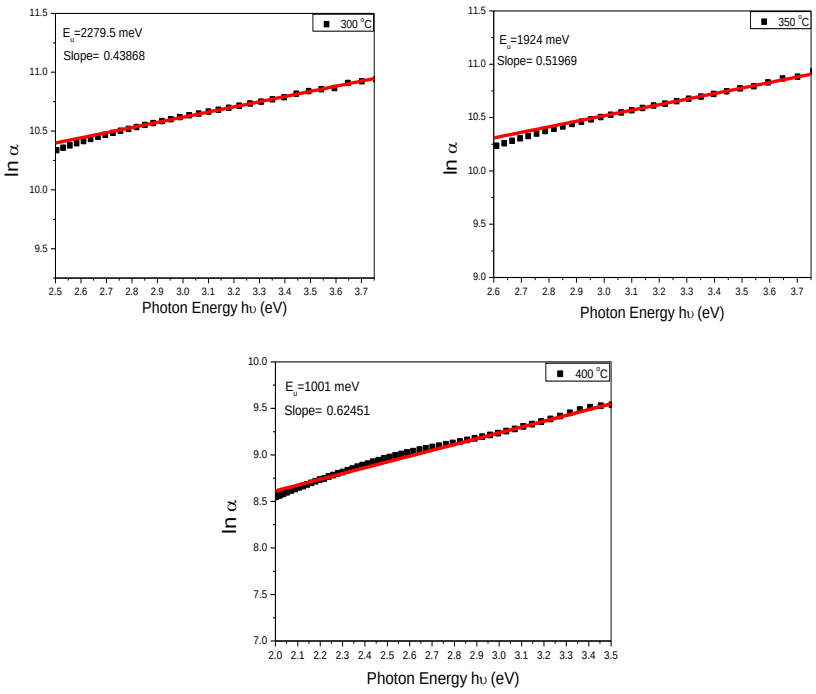

Fig. 5. Urbach energy of Cu_2ZnSnS_4 films at different substrate temperatures.

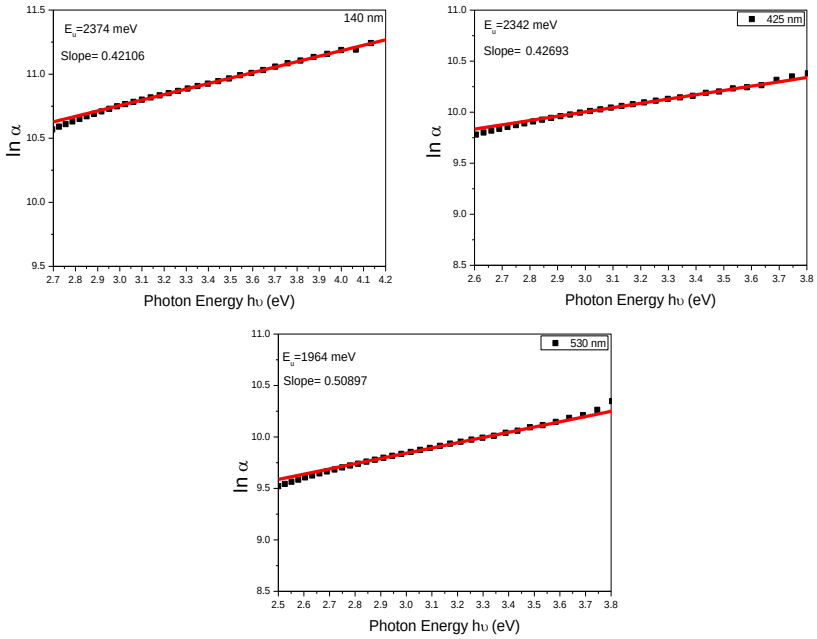

Fig. 6. Urbach energy of Cu_2ZnSnS_4 films at different thicknesses.

The optical energy gap (E_g) was estimated by using Tauc's relation [11]:

$$\alpha h\nu = A'\left(h\nu - E_g\right)^{\mathrm{r}} \tag{4}$$

where: (E_g) is the optical band gap, *A'* is the constant, depending on the structure of the material, while the exponent, *r* depends on the type of transition. In this work, the direct band gap was determined, as shown in Figures (7) and (8). It was noticed that the band gap value decreased when the substrate temperature and thickness increased. This was due to the large number of photons absorbed by the atoms, as shown in Table 3.

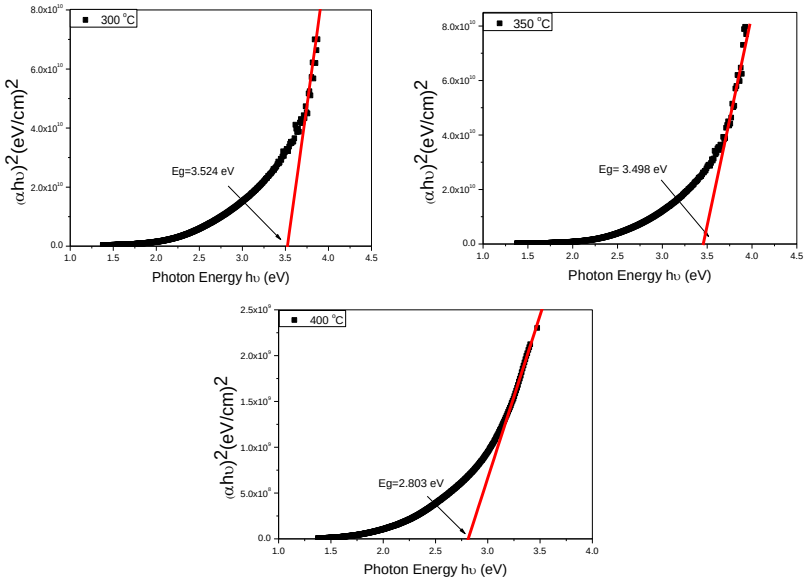

Fig. 7. Tauc's plot of Cu_2ZnSnS_4 films at different substrate temperatures.

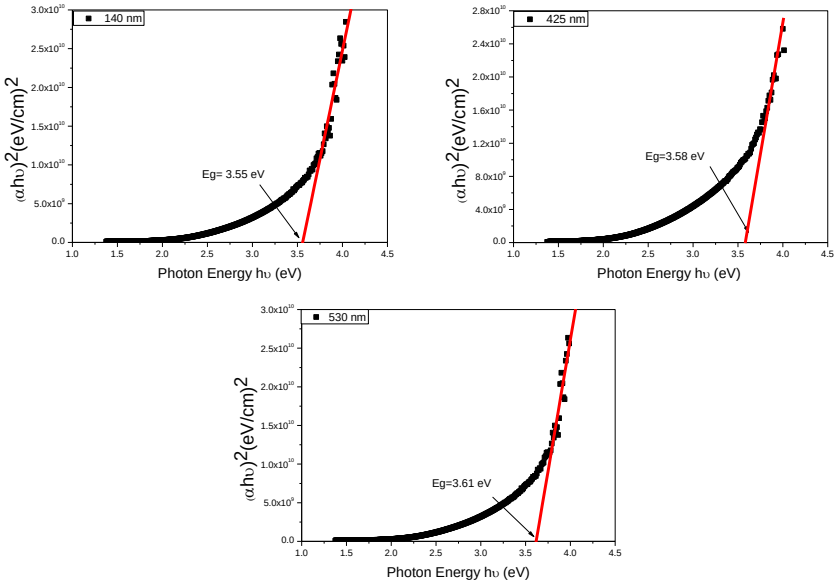

Fig. 8. Tauc's plot of Cu_2ZnSnS_4 films at different thicknesses.

.

Table 3. Energy band gab and Urbach energy of Cu_2ZnSnS_4 films.

Sample	300 °C	350 °C	400 °C	140 nm	425 nm	530 nm
E_g (eV)	3.52	3.49	2.80	3.55	3.58	3.61
E_u (eV)	2279	1924	1001	2374	2342	1964

The extinction coefficient (K_o) was estimated by [11]:

$$K_o = \frac{\alpha\lambda}{4\pi} \tag{5}$$

where λ is the wavelength for the photon incident. Fig. 9 shows K_o against the wavelength. The extinction coefficient (K_o) decreased with substrate temperature and thickness. The lesser value of K_o in the wavelength range of 400 – 900 nm implied that these films very easily absorbed light in this region.

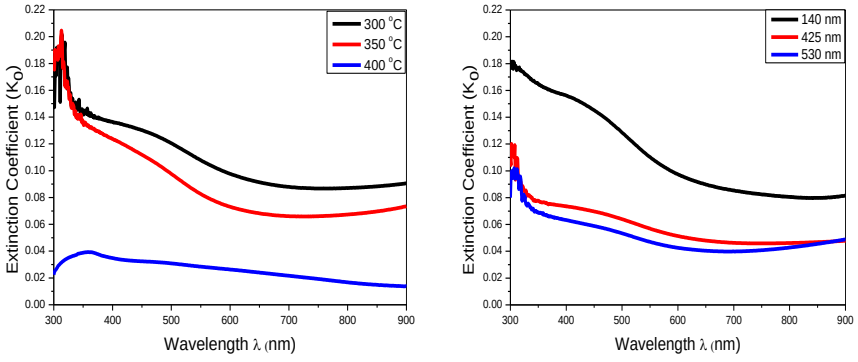

a) *b)*

Fig. 9. Extinction coefficient at various wavelengths of Cu_2ZnSnS_4 (a) at different substrate temperatures, and (b) at different thicknesses.

The dielectric constant was estimated by [11, 13]:

$$\varepsilon = \varepsilon_1 - i\varepsilon_2 \quad (6)$$

where $\varepsilon_1$and ε_2 are the real and imaginary parts, respectively, of the complex dielectric constant. For the estimation of the two parts of the dielectric constant, the following expressions can be used [13, 14]:

$$\varepsilon_1 = n - k^2_o \quad (7)$$

$$\varepsilon_2 = 2nk_o \quad (8)$$

The relationships between the real and imaginary parts of the dielectric constant and photon energy are shown in Figs. 10 and 11. It can be seen that the real and imaginary parts of the dielectric constant decreased with increasing substrate temperature and thickness.

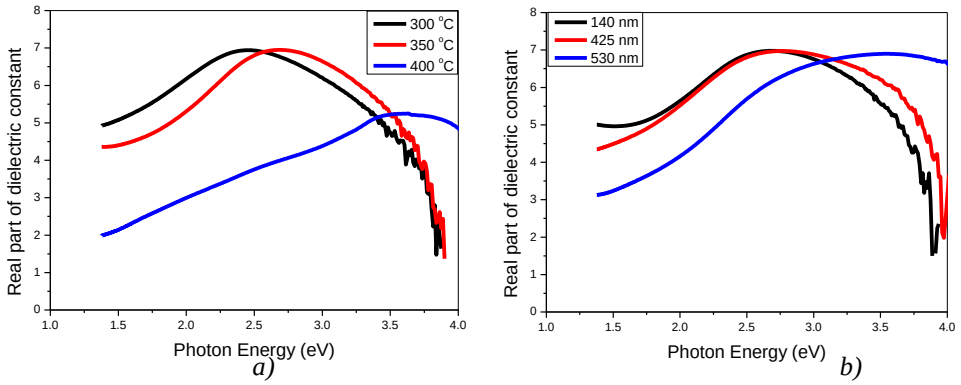

Fig. 10. Real part of dielectric constant as a function of photon energy of Cu_2ZnSnS_4 (a) at different substrate temperatures, and (b) at different thicknesses.

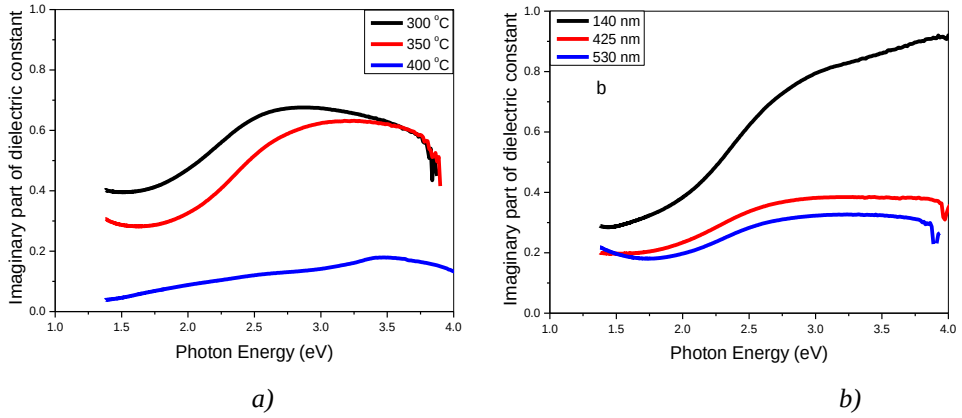

Fig. 11. Imaginary part of dielectric constant as a function of photon energy of Cu_2ZnSnS_4 films (a) at different substrate temperatures, and (b) at different thicknesses.

4. Conclusions

To summarize, this study successfully synthesized Cu_2ZnSnS_4 nanostructures thin films at different substrate temperatures (300, 350 and 400 ^oC) and thicknesses (140, 425 and 530 nm) by using chemical spray pyrolysis. XRD pattern revealed that the deposited films were polycrystalline in nature with a tetragonal structure, and it matched well with the Cu_2ZnSnS_4 structure that had

been previously reported. The T_c value was >1 for all the samples, thus indicating that there were numerous grains in the (112) plane. The transmittance increased with increasing substrate temperature and decreased with increasing thickness. The absorption coefficient was larger than 10^4 cm^{-1}, which denoted the increasing probability of the presence of direct transitions, while the optical energy gap value decreased when the substrate temperature and thickness increased.

References

[1] Qichen Zhao, Ruiting Hao, Sijia Liu, Min Yang, Xinxing Liu, Faran Chang, Yilei Lu, Shurong Wang, Physica B: Condensed Matter **523**(10), 62 (2017).
[2] J. Henry, K. Mohanraj, G. Sivakumar, Journal of Asian Ceramic Societies **4**, 81 (2016).
[3] Prashant K. Sarswat , Michael L. Free, Physica B: Condensed Matter **407**,108 (2012).
[4] H. Katagiri, K. Jimbo, W. Shwe Maw, K. Oishi, M Yamazaki, H. Araki, A. Takeuchi, Thin Solid Films **517**(7), 2455 (2009).
[5] A. M. Saleh , N. A. Bakr, Z. T. Khodair, Digest Journal of Nanomaterials and Bio structures **13**(3), 603 (2018).
[6] Bo Long, Shuying Cheng, Yunfeng Lai, Haifang Zhou, Jinling Yu, Qiao Zheng, Thin Solid Films **5734**, 117 (2014).
[7] Nabeel A. Bakr, Sabah A. Salman, Sabreen A. Hameed, International Journal of Applied Engineering Research **13**(6), 3379 (2018).
[8] Nabeel A. Bakr, Ziad T. Khodair, Hussein I. Mahdi, International Journal of Materials Science and Application **5**(6), 261 (2016).
[9] A. U. Sheleg, V. G. Hurtavy, A. V. Mudryi, M. Ya. Valakh, V. O. Yukhymchuk, I. S. Babichuk, M. Leon, R. Caballero, Semiconductors **48**(10), 1296 (2014).
[10] Ahmed H. Abed, Ziad T. Khodair, Tagreed M. Al-Saadi, Tariq A. Al-Dhahir, AIP Conference Proceedings **2123**, 020019 (2019).
[11] Ziad T. Khodair, Anees A. Khadom, Hassan A. Jasim, Journal of Materials Research and Technology **8**(1), 424 (2019).
[12] Iftikhar M. Ali, Ahmed M. Shano, Nabeel A. Bakr, Journal of Materials Science: Materials in Electronics **29**(13), 11208 (2018).
[13] Ziad T. Khodair, Mushtaq Abed Al-Jubbori, Abdulsalam M. Hassan, Mutaz Salih Aljuboori, Fadhil I. Sharrad, Journal of Electronic Materials **48**(1), 696 (2019).
[14] Ziad T. Khodair, Asaad A. Kamil, Yamamah K. Abdalaah, Physica B **503**, 55 (2016).